SOLID-STATE PULSE COMPRESSION RADARS IN JAPAN

Naoki Anraku[1], Masakazu Wada[1],Hiroshi Yamauchi[2], Ahoro Adachi[2]

[1] TOSHIBA Corporation, Tokyo, Japan,
[2] Meteorological Research Institute(MRI), Tsukuba, Japan,

1. INTRODUCTION

Solid-State Weather Radars (SSWR) have recently gained popularity in Japan because of its capability for pulse shaping, which allows for a precise control of the actual bandwidth usage. Because electromagnetic emission is strictly regulated by the Ministry of Internal Affairs and Communications in Japan, weather radars must minimize their interference to neighboring bands. Since radio is a limited public resource which should be shared efficiently, and the demand for radio communication system is rapidly growing, it is just a matter of time that the bandwidth for weather radar will be also regulated all around the world.

In addition, the use of solid-state based weather radar promises lower peak power, which reduces the operational costs of the weather radar, as the financial burden is directly proportional to the peak power level in Japan. Using long transmit waveform and pulse compression, weather radars can achieve similar sensitivity performance to a high-power system, while linear solid-state amplifiers allows for minimal electromagnetic interference. In a joint effort between Toshiba Corporation and the Meteorological Research Institute (MRI), we developed the parabolic dish-type C-band SSWR, which is currently installed at the MRI research facility in Tsukuba, Japan, in order to study the efficacy of a weather radar system using solid-state transmitter.

Recently, we implemented the nonlinear frequency modulation (NLFM) waveform, which was developed by the Advanced Radar Research Center (ARRC) of Oklahoma University (OU). The Optimized Frequency Modulation (OFM) waveform such as NLFM does not require mismatch filtering and, thus, increases the system sensitivity compared to a mismatched filtering pulse compression technique. In this paper, we will introduce result of experiment performed in early September 2013.

2. C-BAND SOLID-STATE WEATHER RADAR

In 2007, Toshiba installed a SSWR system at the MRI which was the first SSWR system used in Japan(Wada et al, 2009). General characteristics of SSWR are high-accuracy, small size, easier maintenance, low lifecycle cost, and low spurious emission. Through observation at the MRI, C-band SSWR proved to have sufficient capability to observe heavy rainfall with practical scanning rate. The peak values of Rho_{HV} and the standard deviation of Phi_{DP} for stratiform rain were 0.998 and 1.0° (Yamauchi et al, 2012) Figure 1 shows the appearance of C-band SSWR in MRI facility and Figure 2 shows its major components. Table I. shows the major specification of C-band SSWR installed at the MRI.

Figure1.C-band SSWR installed in the MRI facility

Figure 2. C-band Solid-State Weather Radar

Table 1: SPECIFICATION OF C-BAND SOLID-STATE WEATHER RADAR INSTALLED IN THE MRI

Item	Description
Observation range	230 km or more in radius
Frequency	5370 MHz
Pulse width	1 μs to 129 μs
Peak Power	3.5 kW per polarization
Receiver dynamic range	110 dB
Radome diameter	7 m or less
Antenna diameter	4 m or less
Antenna gain	42 dBi or more
Beam width	1 deg or less
Range resolution	150 m or less
Radar products	Reflectivity (Z_H, Z_V)
	Differential Reflectivity (Z_{DR})
	Doppler velocity V (m/s)
	Spectrum width W (m/s)
	Differential phase Φ_{DP} (deg)
	Specific differential phase (K_{DP})
	Correlation coefficient (ρ_{HV})
Manufacture	Toshiba Corporation

3. NON-LINEAR FREQUENCY MODULATION

A waveform with non-linear frequency modulation (NLFM) was used. It should be noted that a minimal tapering is still being used for the transmit pulse shape in order to reduce interference to neighboring bands. Briefly, the waveform is optimized through an interactive process by adjusting the frequency chirp pattern until convergence to the desired performance metrics. A user-specified amplitude tapering is applied in the waveform synthesis step in order to minimize abrupt amplitude change in hardware. During the optimization process, a continuous chirp function is adjusted at each iteration, the corresponding waveform is synthesized and evaluated for the performance, which include several measurements on the ambiguity function of the waveforms, e.g., 3-dB resolution, peak sidelobes, etc. In the end, a waveform that simultaneously satisfies all the desired performance parameters are obtained, if achievable. The optimized waveform will be referred to as the optimized frequency modulation (OFM) herein. It should be emphasized here that the pulse compression scheme of the waveform is set to be match filtering so that the SNR is maximized. As such, there is no need for additional windowing at the later processing, which is advantageous compared to the windowed LFM method.

4. PERFORMANCE OF EACH FM IN LOOPBACK TEST

We had originally used the Blackman-Harris window function for improving range-sidelobe which appeared when received long FM pulse is compressed in pulse compression process.

The Blackman-Harris window function with LFM has strong advantage in reducing range-sidelobe,and using raised cosine is very effective for suppressing range sidelobe (Nakagawa et al 2005) however, there is a disadvantage in power efficiency and sensitivity; that is window function process loss and raised cosine loss. From our experience, 60 dB of range-sidelobe reduction is sufficient for weather observation. The expectation for using NLFM is eliminating the window function process loss with reduction of more than 60 dB of range-sidelobe.

We performed loop-back tests with MRI radar to make a comparison between LFM with Blackman-Harris window, and NLFM with no window as test case 1. A list of the original parameters, which was a Blackman-Harris window with LFM, is given in TABLE II, and a list of the testing parameters, which uses NLFM, is given in TABLE III. Figure 3 and Figure 4 shows theoretical waveforms of test case 1. Also, for objective comparison, we performed loop-back tests of LFM with no-window function and NLFM with no-window function which uses 2%, 5% and 10% raised cosine, as test case 2. Figure 5 to Figure 10 shows theoretical waveforms of test case 2.

Theoretical result proves both LFM and NLFM have capability to achieve necessary performances.

Table 2: ORIGINAL LFM WAVEFORM PARAMETERS

| Parameter	Value
Modulation	LFM
Chirp type	Up Chirp
Raised cosine	10 %
Pulse width	111 us
Sampling frequency	2 MHz (Ref), 80 MHz (Drive)
Center frequency	0 MHz (Ref), 20 MHz (Drive)
Window function	Blackman-Harris
Range resolution(3dB)	150m

Table 3: NLFM WAVEFORM PARAMETERS

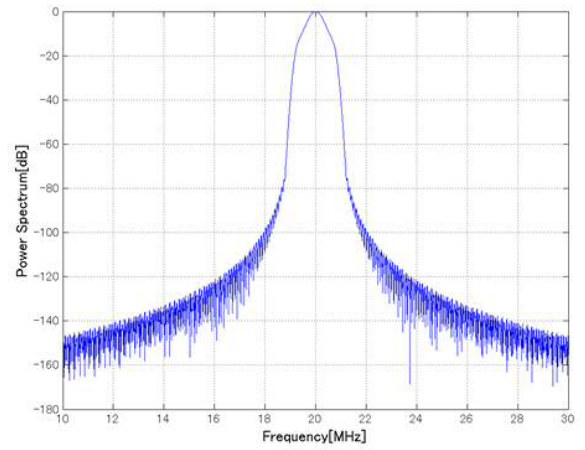| Parameter	Value
Modulation	NLFM
Chirp type	Down Chirp
Raised cosine	10 %
Pulse width	111 us
Sampling frequency	2 MHz (Ref), 80 MHz (Drive)
Center frequency	0 MHz (Ref), 20 MHz (Drive)
Window function	-
Range resolution(3dB)	150m
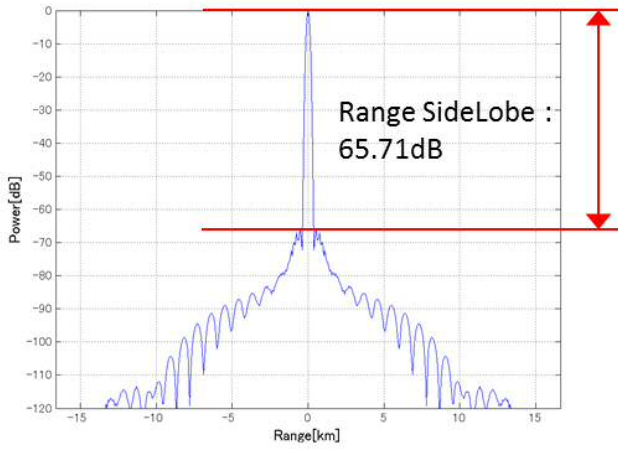
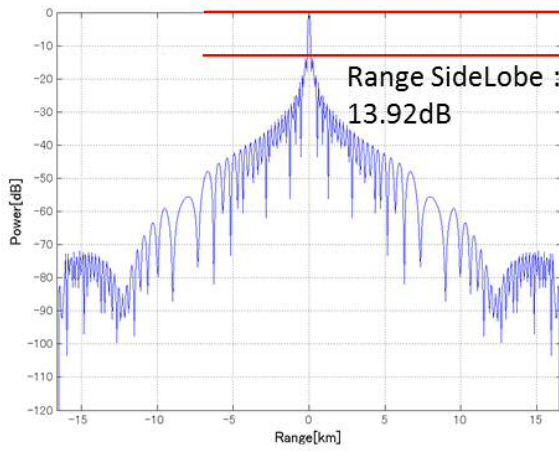3(a) Compressed waveform
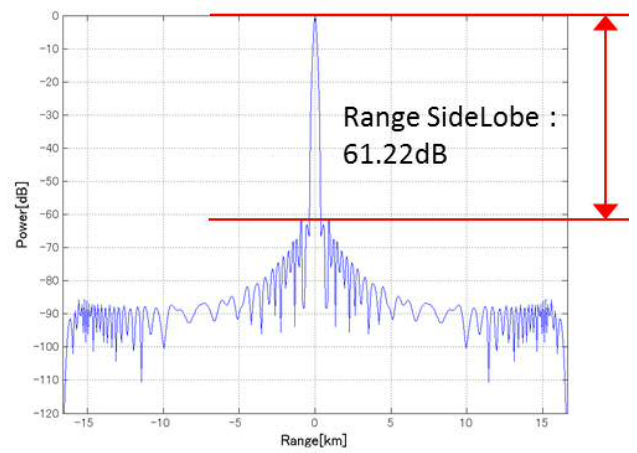
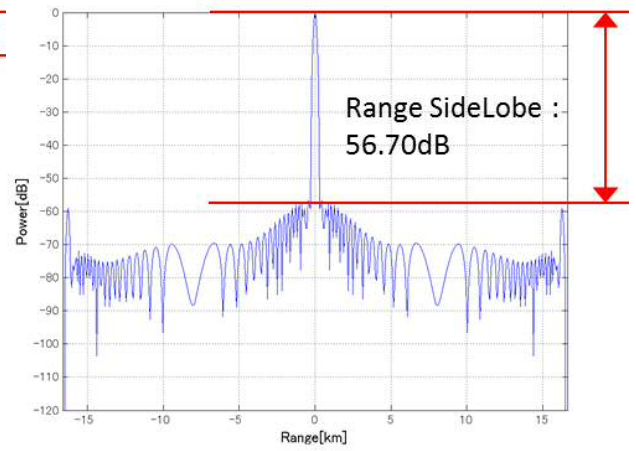4(a) Compressed waveform
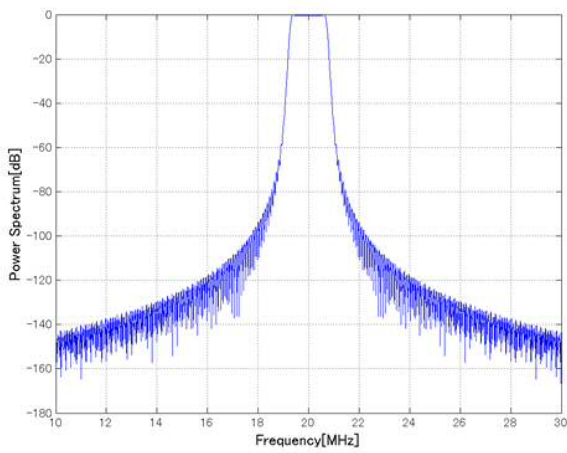
3(b) Power Spectrum

4(b) Power Spectrum

Figure 3: Original LFM waveform
(theoretical data)
LFM, Raised Cosine 10%,
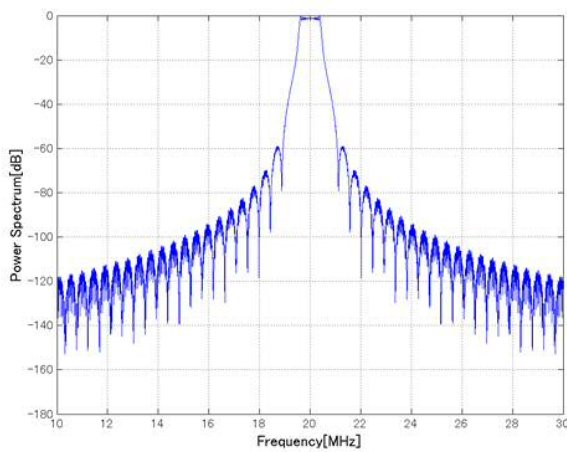Swept bandwidth 1.63MHz
Blackman-Harris window

Figure 4: NLFM waveform
(theoretical data)
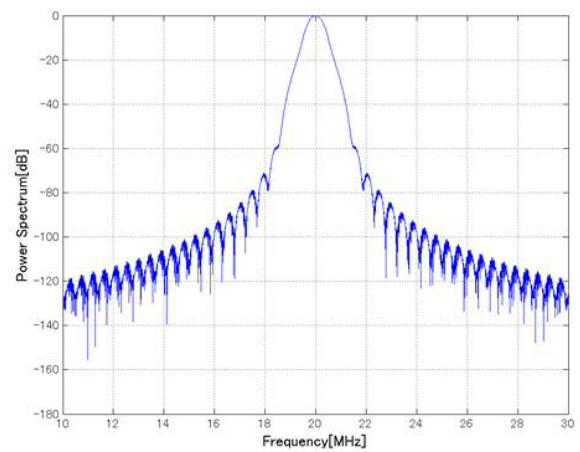NLFM, Raised Cosine 10%,
Swept bandwidth 1.63MHz
No-window

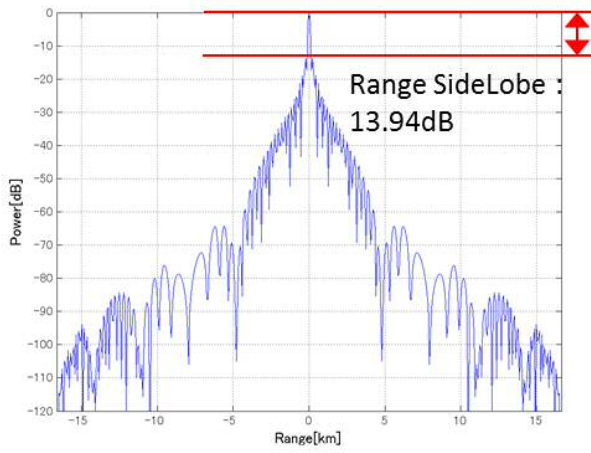5(a)   Compressed waveform

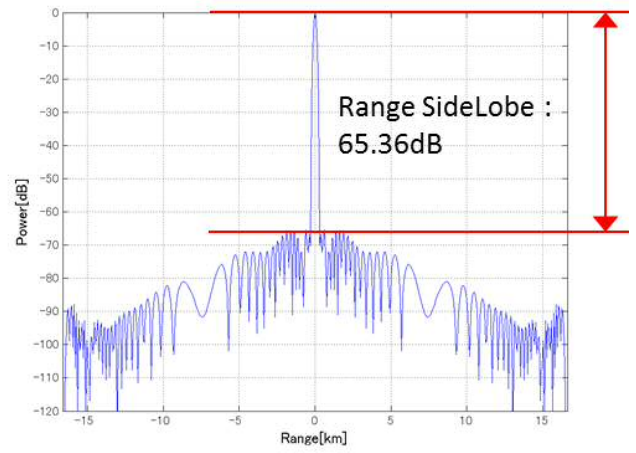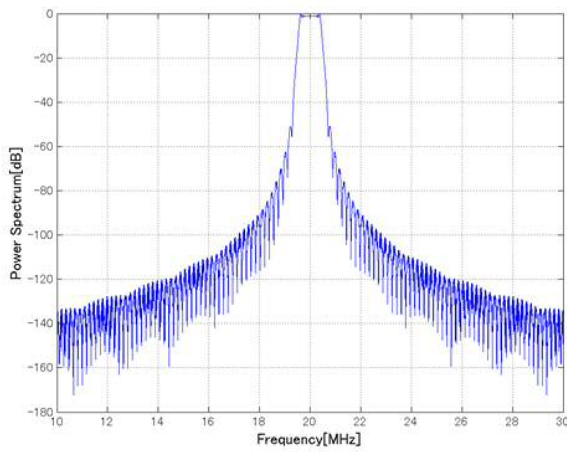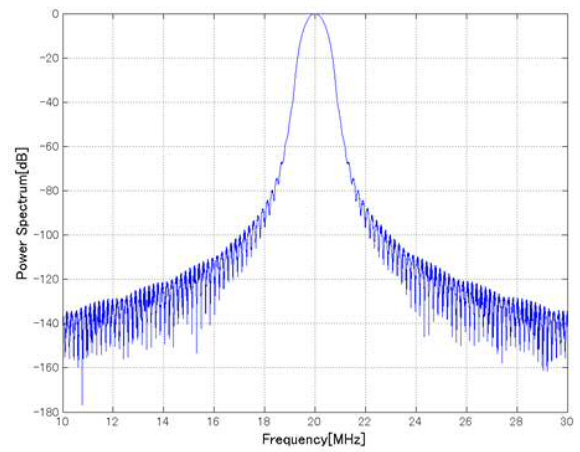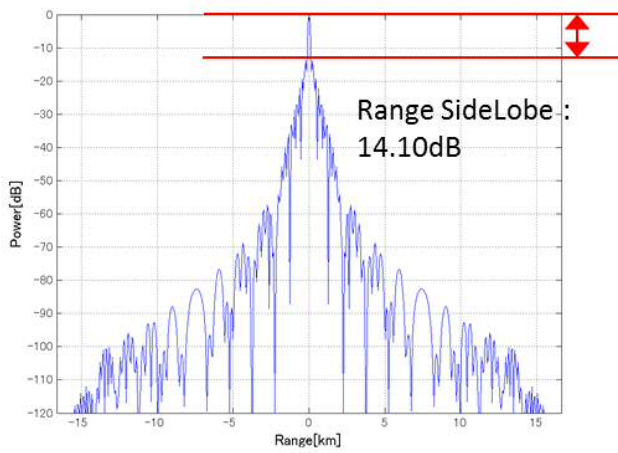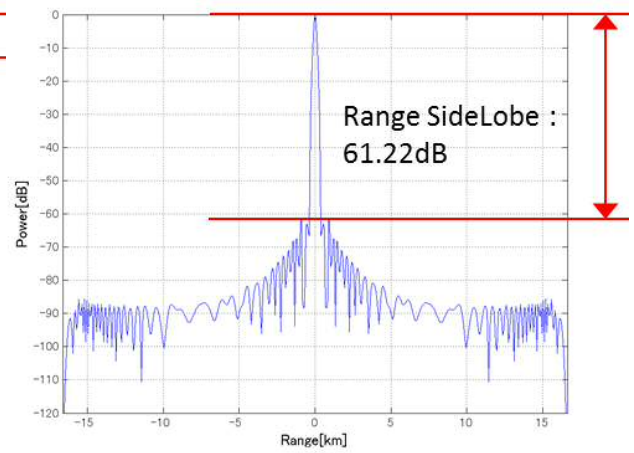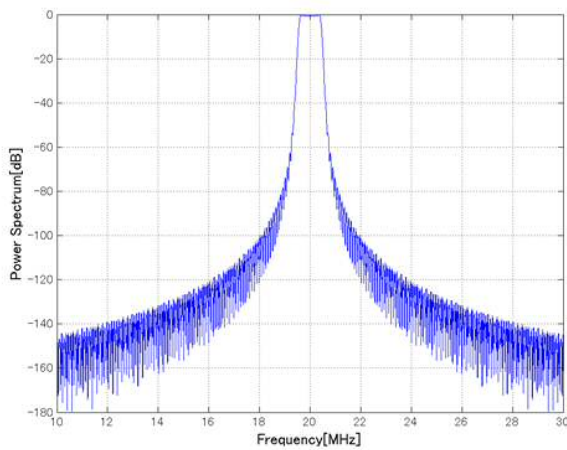6(a)   Compressed waveform

5(b)   Power Spectrum

6(b)   Power Spectrum

Figure 5: LFM waveform
(theoretical data)
LFM, Raised Cosine 2%,
Swept bandwidth 0.91MHz
No-window

Figure 6: NLFM waveform
(theoretical data)
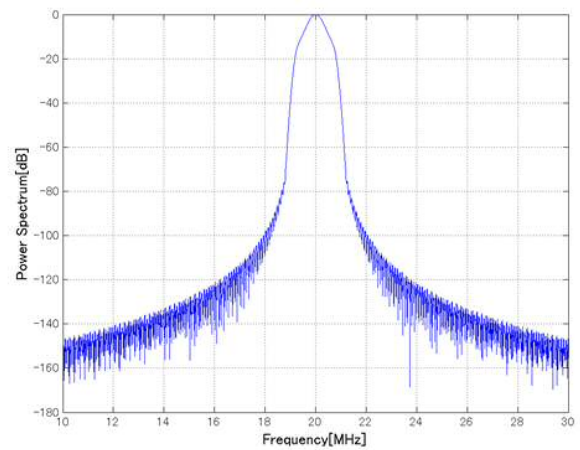NLFM, Raised Cosine 2%,
Swept bandwidth 1.63MHz
No-window

4

7(a)   Compressed waveform   8(a)   Compressed waveform

7(b)   Power Spectrum   8(b)   Power Spectrum

Figure 7: LFM waveform
(theoretical data)
LFM, Raised Cosine 5%,
Swept bandwidth 0.94MHz
No-window

Figure 8: NLFM waveform
(theoretical data)
NLFM, Raised Cosine 5%,
Swept bandwidth 1.63MHz
No-window

9(a)　Compressed waveform

10(a)　Compressed waveform

9(b)　Power Spectrum

10(b)　Power Spectrum

Figure 9: LFM waveform
(theoretical data)
LFM,Raised Cosine 10%,
Swept bandwidth 1.00MHz,
No-window

Figure 10: NLFM waveform
(theoretical data)
NLFM, Raised Cosine 10%,
Swept bandwidth 1.63MHz
No-window
(same as Figure.4)

5. RESULT OF LOOP-BACK TEST(CASE 1)

(1) Original LFM waveform
With these parameters, we had achieved peak sidelobe level of -68.49dB, and -78.09 dB of Spurious Emission ±5MHz outside of center frequency, with 0.58dB Transmission loss and 2.56 dB window function loss.

(2) NLFM waveform
LFM waveform achieved peak sidelobe level of -62.46dB, and -78.18 dB of Spurious Emission ±5MHz outside of center frequency, with 0.58dB Transmission loss.
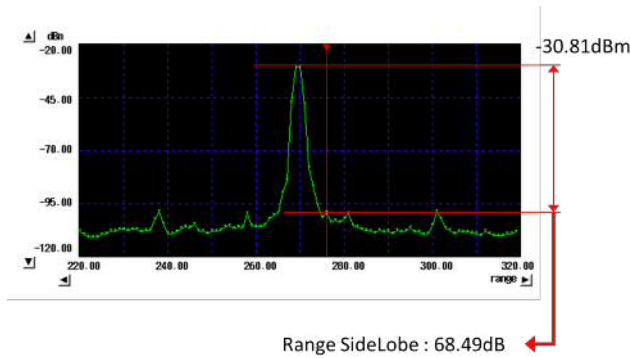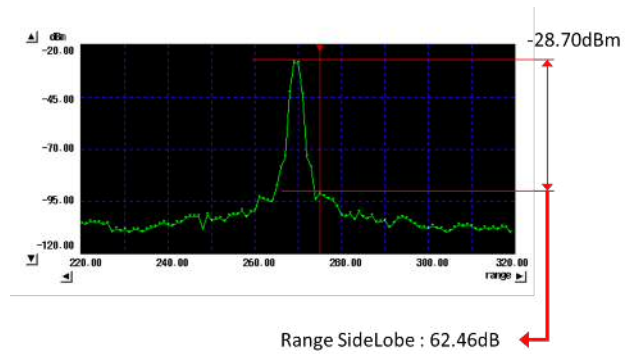

Figure 11: Result of Original LFM waveform (loop-back)
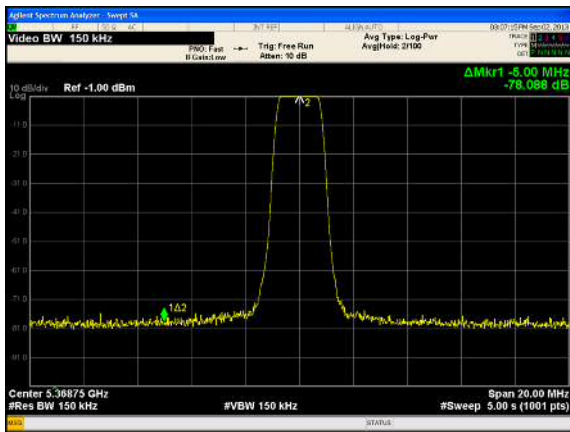

Figure 13: Result of NLFM waveform (loop-back)

Figure 12: Result of Original LFM waveform (loop-back)
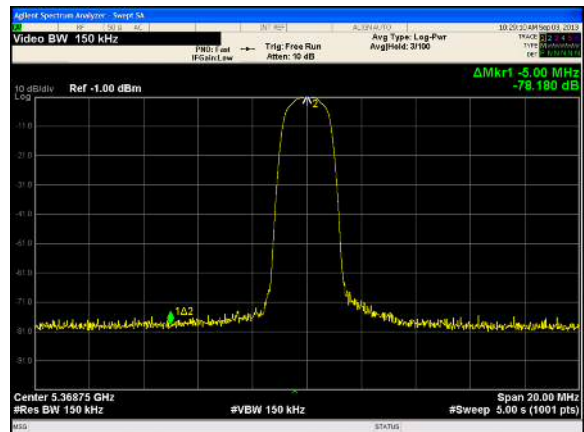

Figure 14: Result of NLFM waveform (loop-back)

Table 4: OVERALL TEST RESULT OF CASE 1

Pattern	1	2
Modulation	LFM	NLFM
Chirp type	Up	Down
Swept BW (MHz)	1.63	1.63
Peak sidelobe level (dB)	-68.49	-62.46
Spurious Emission ±5MHz outside of F_0 (dB)	-78.09	-78.18
Transmission loss (dB)	0.58	0.58

6. RESULT OF ACTUAL OBSERVATION (CASE 1)

By using MRI radar, we observed weather phenomena with NLFM. Figure 15 shows the September 4th 2013 rain event near Tsukuba, Japan. From the south side, convective rainfall is observed.
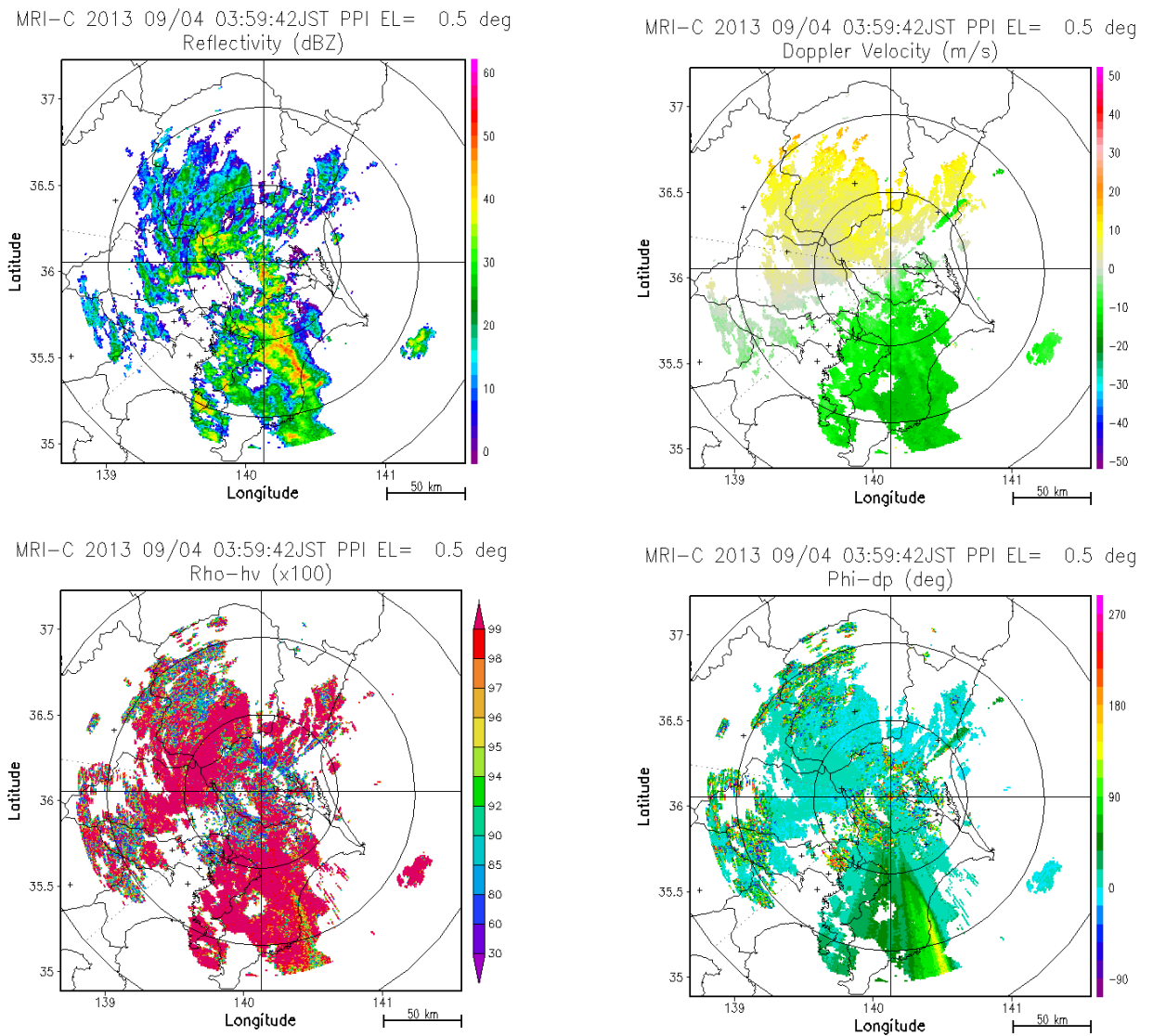

Figure 15: Actual observation data by using NLFM waveform, Raised Cosine 10%, Swept bandwidth 1.63MHz, No-window.

7. RESULT OF LOOP-BACK TEST(CASE 2)

In addition to NLFM vs. LFM with Blackman-Harrison window in both 10% raised cosine, we performed experiments of 2%, 5% and 10% raised cosine for both NLFM and LFM with no-window. TALBE 5 shows common parameters for all waveform. TALBE 6 and TALBE 7 show overall result of Test Case2. Figure 16 and Figure 17 shows actual test data taken from radar system. These results show that NLFM has higher capability in reducing peak sidelobe levels, and LFM has high capability in suppressing spurious emissions around center frequency.

Table 5:   WAVEFORM COMMON PARAMETERS

| Parameter	Value
Pulse width	111 us
Sampling frequency	2 MHz (Ref), 80 MHz (Drive)
Center frequency	0 MHz (Ref), 20 MHz (Drive)
Range resolution(3dB)	150m

Table 6:   OVERALL TEST RESULT OF CASE 2 (1/2)

Pattern	1	2	3
Modulation	LFM	LFM	LFM
Chirp type	Up	Up	Up
Swept BW (MHz)	0.91	0.94	1.00
Raised Cosine (%)	2	5	10
Peak sidelobe level (dB)	-22.20	-23.28	-25.70
Spurious Emission ±5MHz outside of F_0 (dB)	-80.41	-79.91	-80.82
Transmission loss (dB)	0.11	0.28	0.58

Table 7:   OVERALL TEST RESULT OF CASE 2 (2/2)

| Pattern	4	5	6
Modulation	NLFM	NLFM	NLFM
Chirp type	Down	Down	Down
Swept BW (MHz)	1.63	1.63	1.63
Raised Cosine (%)	2	5	10
Peak sidelobe level (dB)	-51.01	-47.55	-62.46
Spurious Emission ±5MHz outside of F_0 (dB)	-78.88	-78.76	-78.18
Transmission loss (dB)	0.11	0.28	0.58
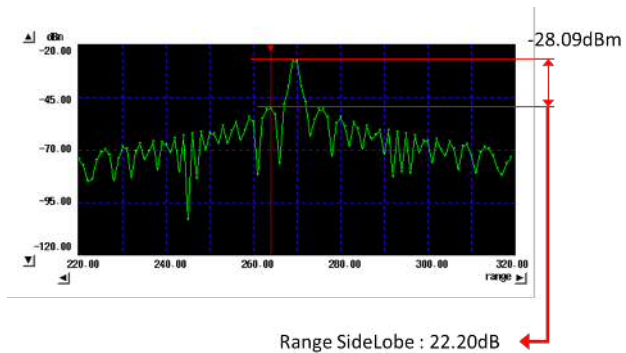
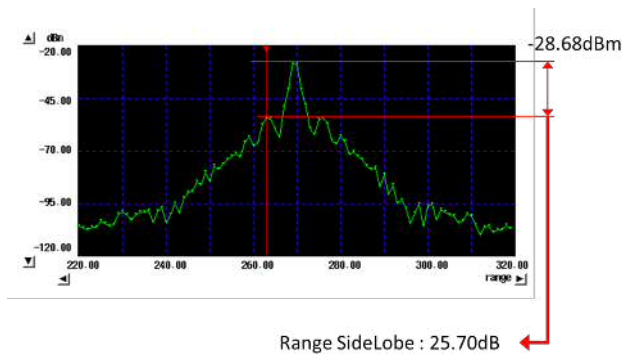Pattern1: LFM, Raised Cosine 2%,
Swept bandwidth 0.91MHz
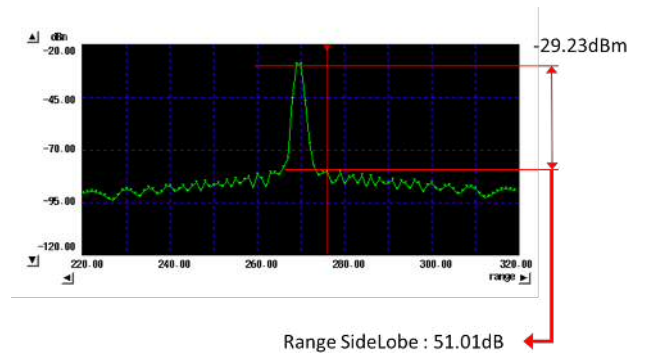
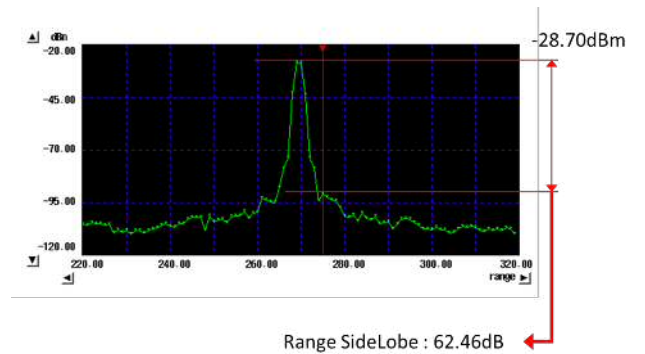Pattern4: NLFM, Raised Cosine 2%,
Swept bandwidth 1.63MHz
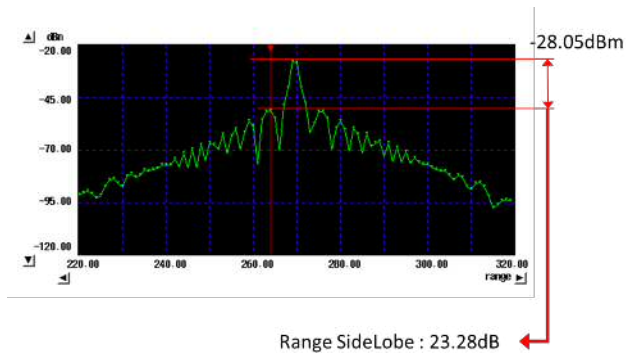
Pattern2: LFM, Raised Cosine 5%,
Swept bandwidth 0.94MHz
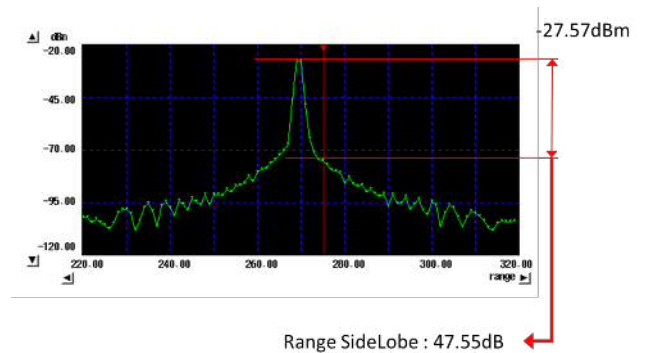
Pattern5: NLFM, Raised Cosine 5%,
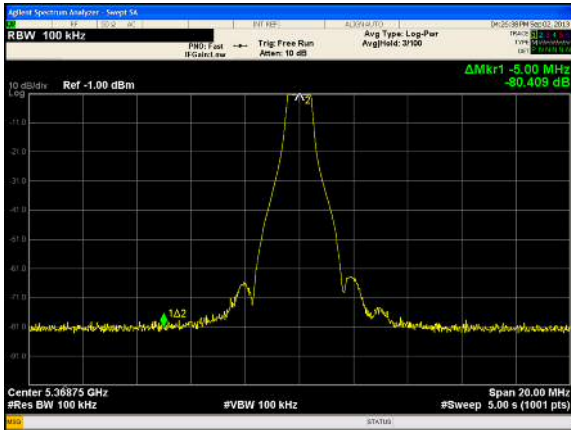Swept bandwidth 1.63MHz

Pattern3: LFM, Raised Cosine 10%,
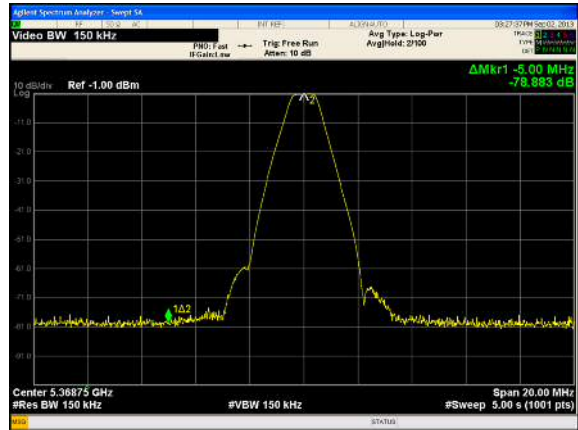Swept bandwidth 1.00MHz

Pattern6: NLFM, Raised Cosine 10%,
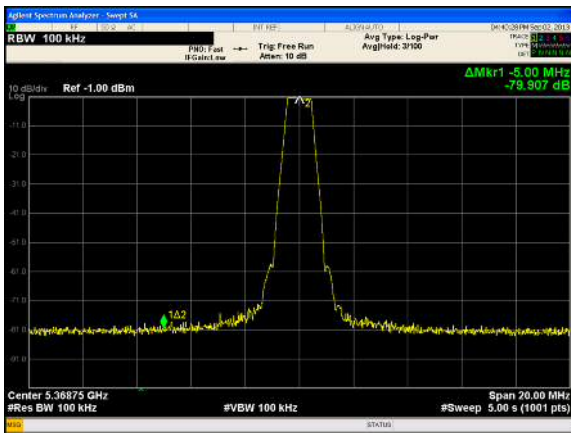Swept bandwidth 1.63MHz

Figure 16: Result of Loop-back test, showing range resolution of each waveforms.
Because we set 150m renge resolution as restraint condition, we maintained swept
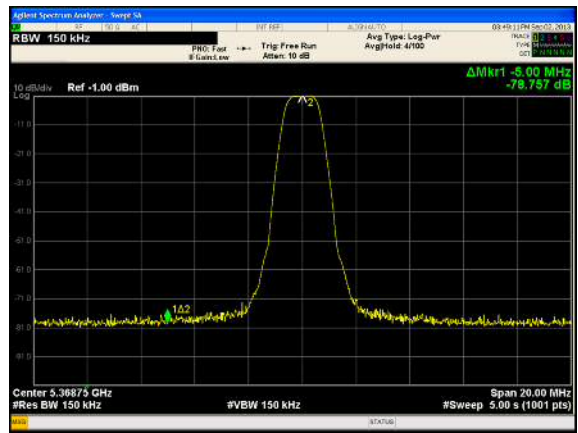bandwidth to keep same condtion for LFM and NLFM.

Pattern1: LFM, Raised Cosine 2%,
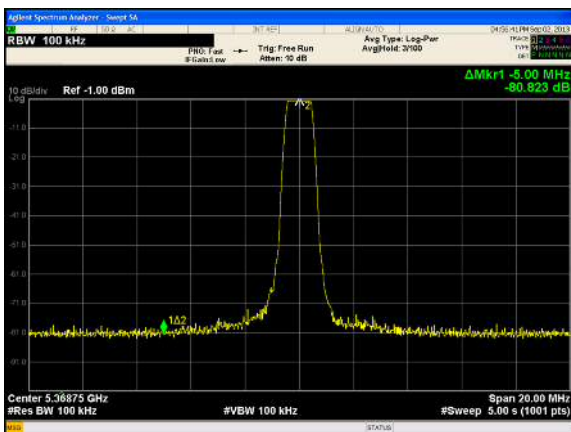Swept bandwidth 0.91MHz

Pattern4: NLFM, Raised Cosine 2%,
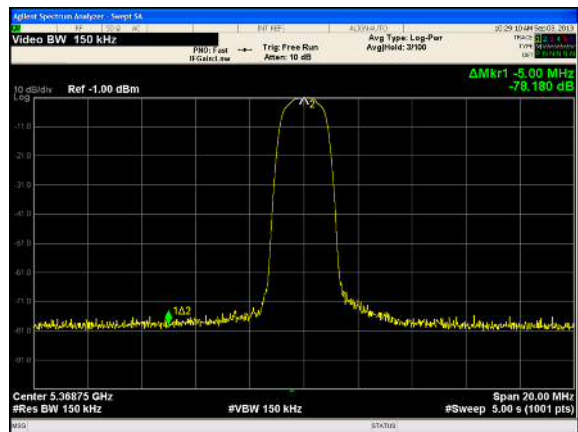Swept bandwidth 1.63MHz

Pattern2: LFM, Raised Cosine 5%,
Swept bandwidth 0.94MHz

Pattern5: NLFM, Raised Cosine 5%,
Swept bandwidth 1.63MHz

Pattern3: LFM, Raised Cosine 10%,
Swept bandwidth 1.00MHz

Pattern6: NLFM, Raised Cosine 10%,
Swept bandwidth 1.63MHz

Figure 17: Result of Loop-back test, showing fequency spectrum of each waveforms.
Because we set 150m range resolution as restraint condition, we maintained swept
bandwidth to keep same condtion for LFM and NLFM.

8. CONCLUSION AND FUTURE WORK

A description of experimental results was presented in this paper. The sensitivity of radar was improved by using NLFM with sufficient range-sidelobe reduction (more than 60dB). Moreover, the nature of Solid-State weather radar, and "Made in Japan quality" produced results approaching the theoretical level.

The waveform optimization technique developed by ARRC-OU has the ability to build in pre-distortion into the design for hardware optimization (Kurdzo et al 2013). Additional improvements can be expected with the hardware response included in the optimization process. For future development, we will apply the pre-distortion function to MRI radars to further improve the waveform performance. Also, we are planning to apply the OFM technique to Phased-Array Weather Radars.

REFERENCES

Nakagawa, K., Hanado, H., Fukutani, K., and Iguchi, T., 2005: Development of a C-band pulse compression weather radar. extended abstract, 32nd Conf. on Radar Meteorology, Albuquerque, U.S, Amer. Meteor. Soc.., P12R.11.

Wada, M., Horikomi, J., and Mizutani, F., 2009: Development of solid-state weather radar. preprints, 34th Conf. on Radar Meteorology, Williamsburg, VA, U.S, Amer. Meteor. Soc., 12B.4.

Yamauchi, H., Adachi A., Suzuki O., and Kobayashi T., 2012:Precipitation estimate of a heavy rain event using a C-band solid-state polarimetric radar, ERAD 2012, The 7th European conference on radar in meteorology and hydrology.

Kurdzo, J. M., B. L. Cheong, R. D. Palmer, G. Zhang, and J. B. Meier, 2013: A pulse compression waveform for improved-sensitivity weather radar observations. Journal of Atmospheric and Oceanic Technology, (under review).